Supporting information

Synthesis and Characterization of $[Ru(NC^{NHC}O)(bpy)L]^+$ Complexes and Their Reactivity towards Water Oxidation

Fanglin Cai, [†[a]] *Wei Su,*[†] [a] *Hussein A. Younus,* [d] *Kui Zhou,* [a] *Cheng Chen,* [a] *Somboon Chaemchuen* [a] *and Francis Verpoort**[a, b, c]

[a] State Key Laboratory of Advanced Technology for Materials Synthesis and Processing, Wuhan University of Technology, Wuhan 430070 (P.R. China)

[b] National Research Tomsk Polytechnic University, Lenin Avenue 30, 634050 Tomsk (Russian Federation)

[c] Ghent University, Global Campus, Songdo, Ywonsu-Gu, Incheon (Republic of Korea)

[d] Chemistry Department, Faculty of Science, Fayoum University, Fayoum 63514 (Egypt)

E-mail: francis.verpoort@ugent.be

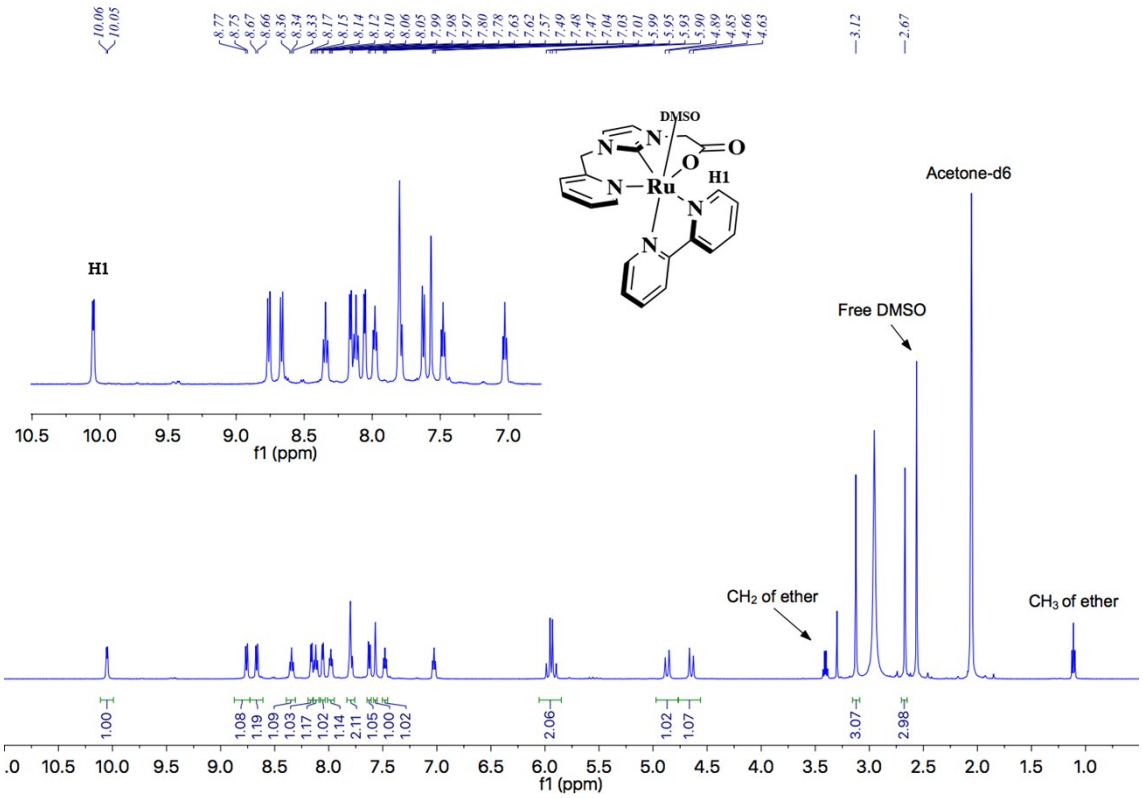

Figure S1. ^{1}H NMR spectrum of complex **1** in acetone-d_6 at 298 K.

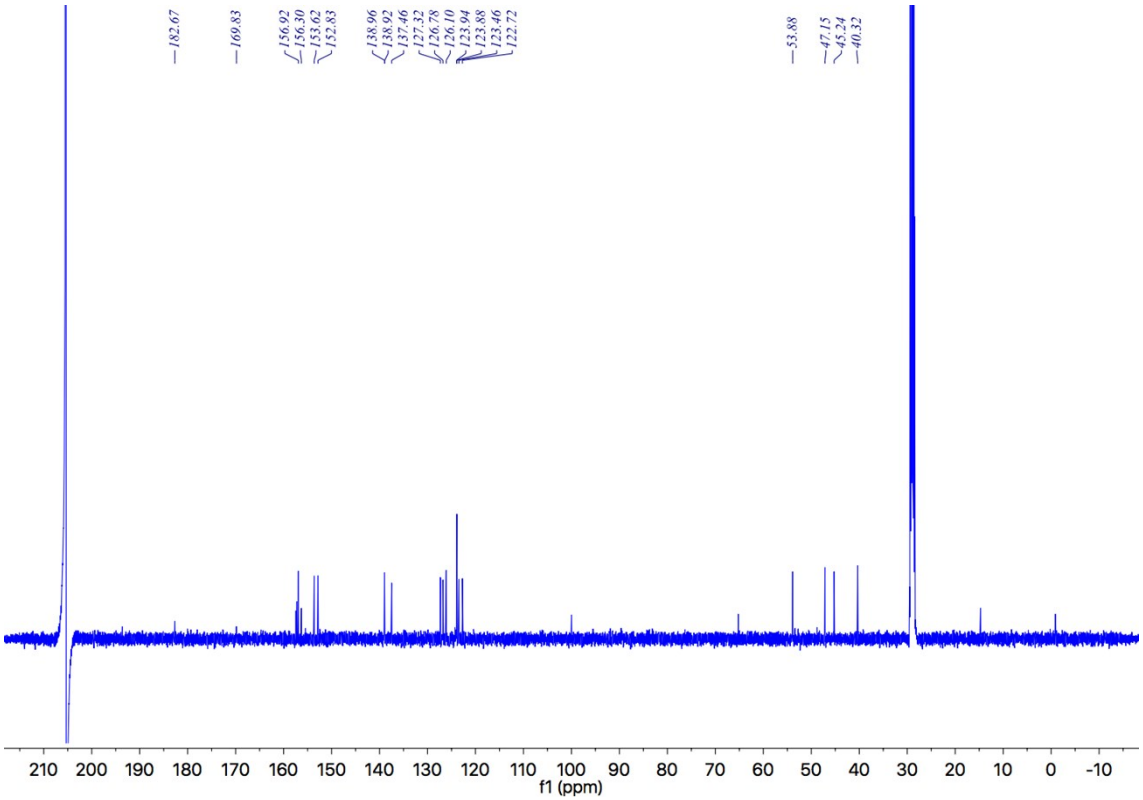

Figure S2. ^{13}C NMR spectrum of complex **1** in acetone-d_6 at 298 K.

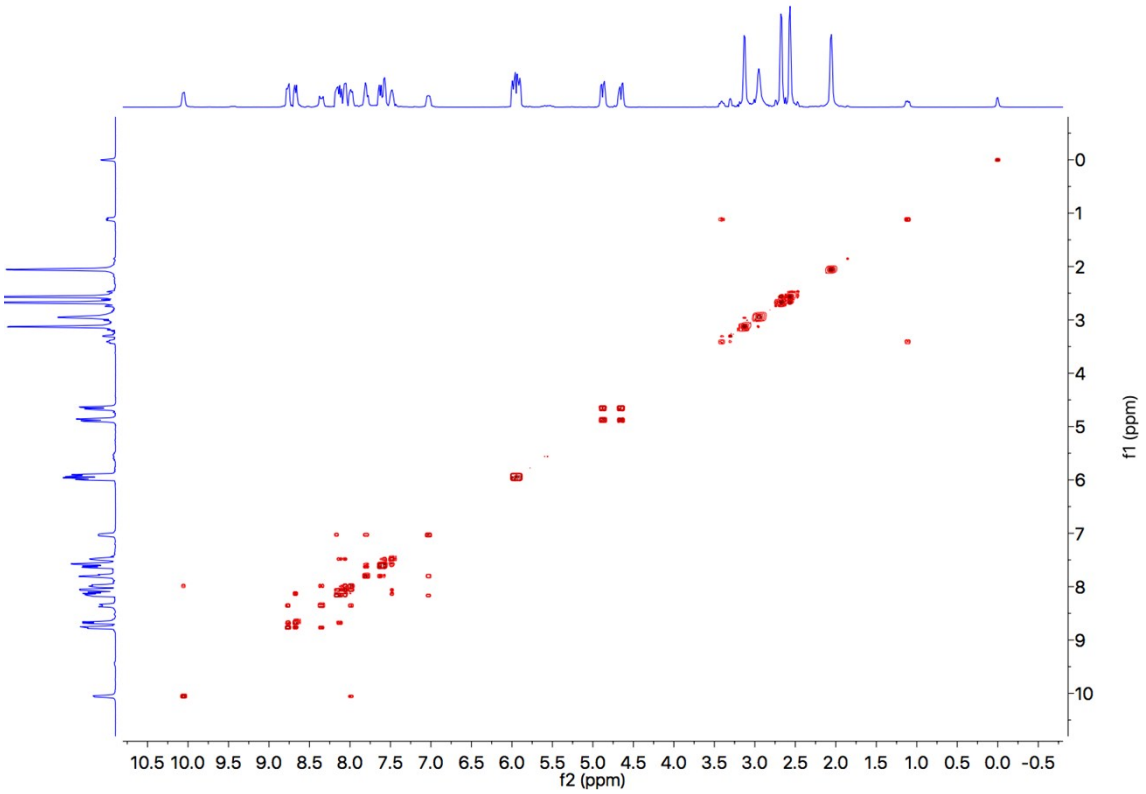

Figure S3. H-H COSY NMR spectrum of complex **1** in acetone-d_6 at 298 K.

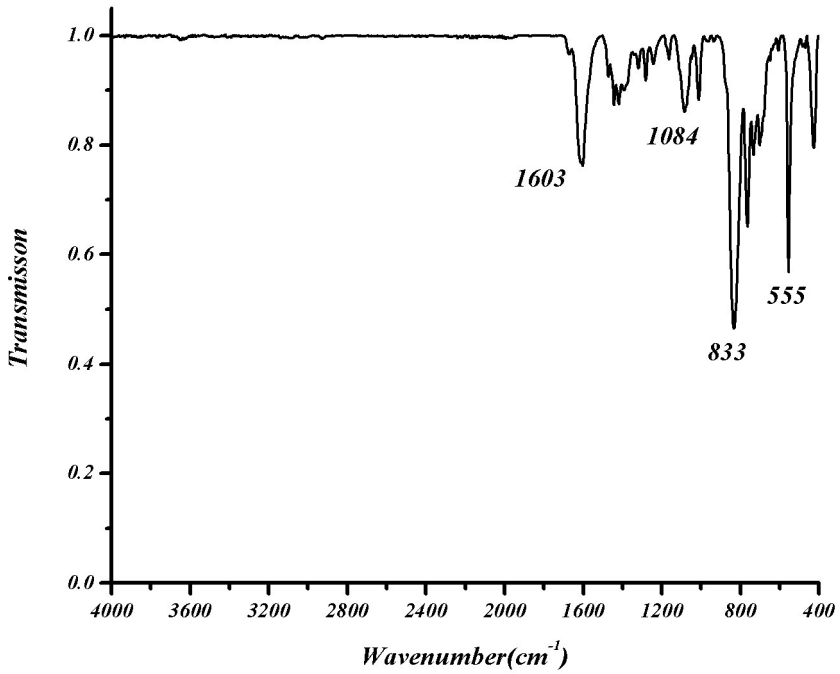

Figure S4. FT-IR of complex **1**.

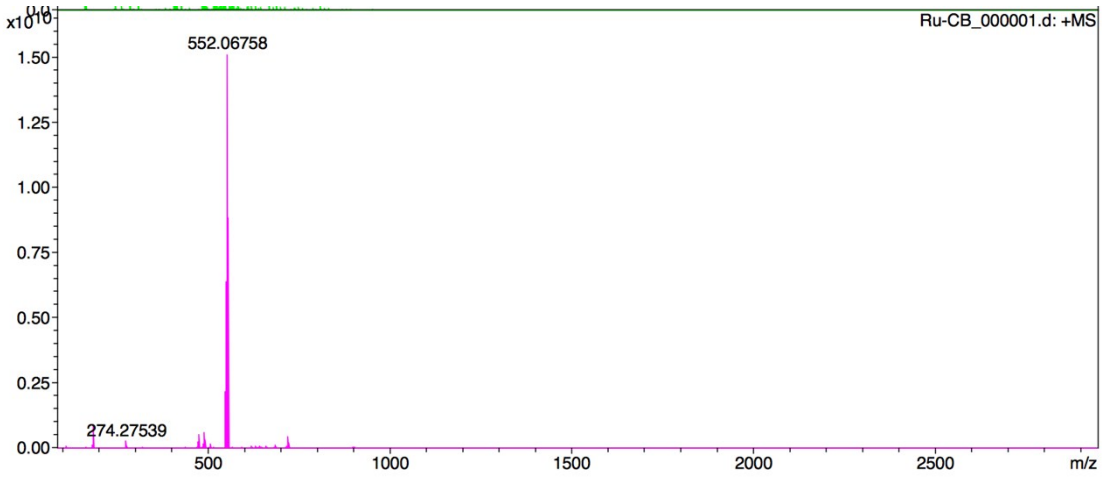

Figure S5. Mass spectrum of complex **1** in H_2O at positive mode.

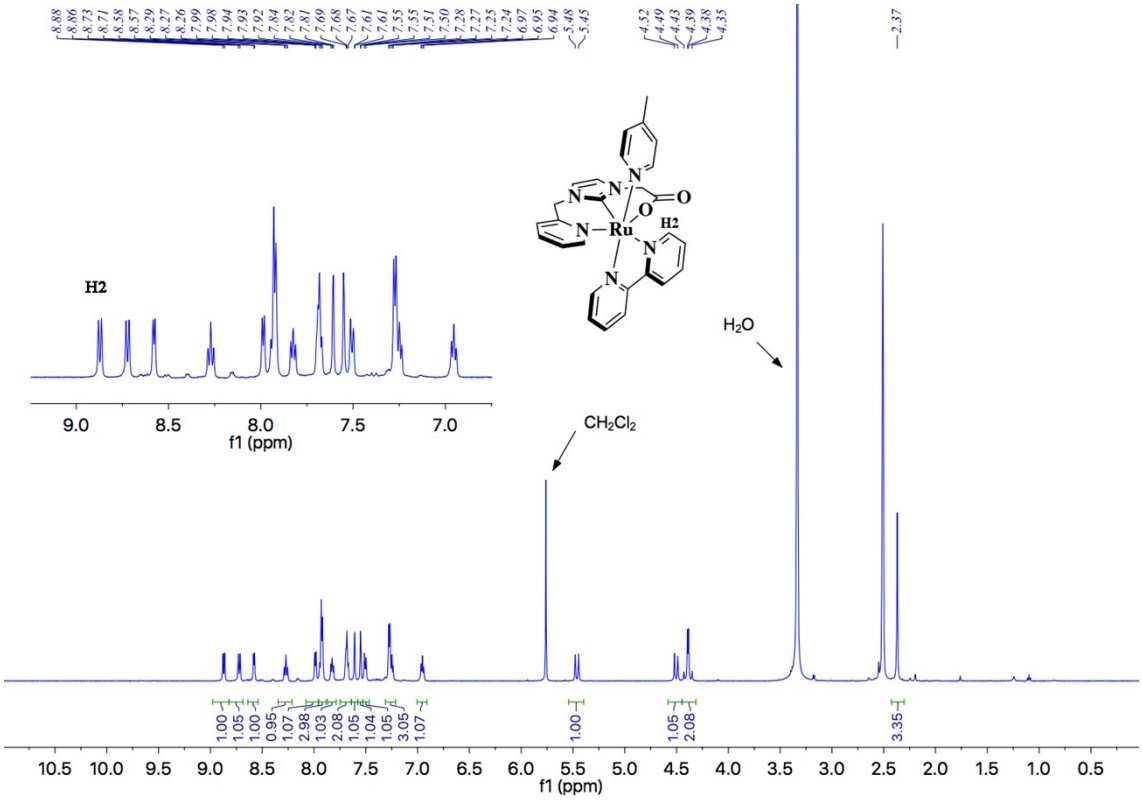

Figure S6. ^{1}H NMR spectrum of complex **2** in DMSO-d_6 at 298 K.

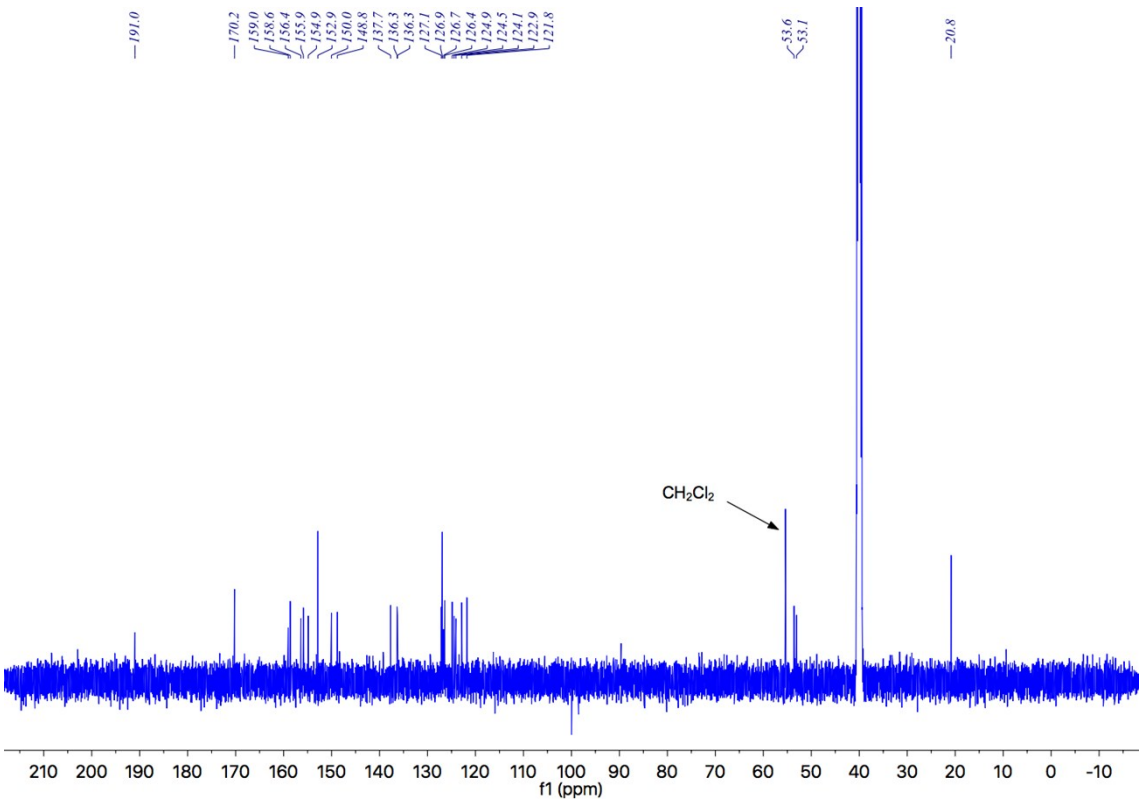

Figure S7. ^{13}C NMR spectrum of complex **2** in DMSO-d_6 at 298 K.

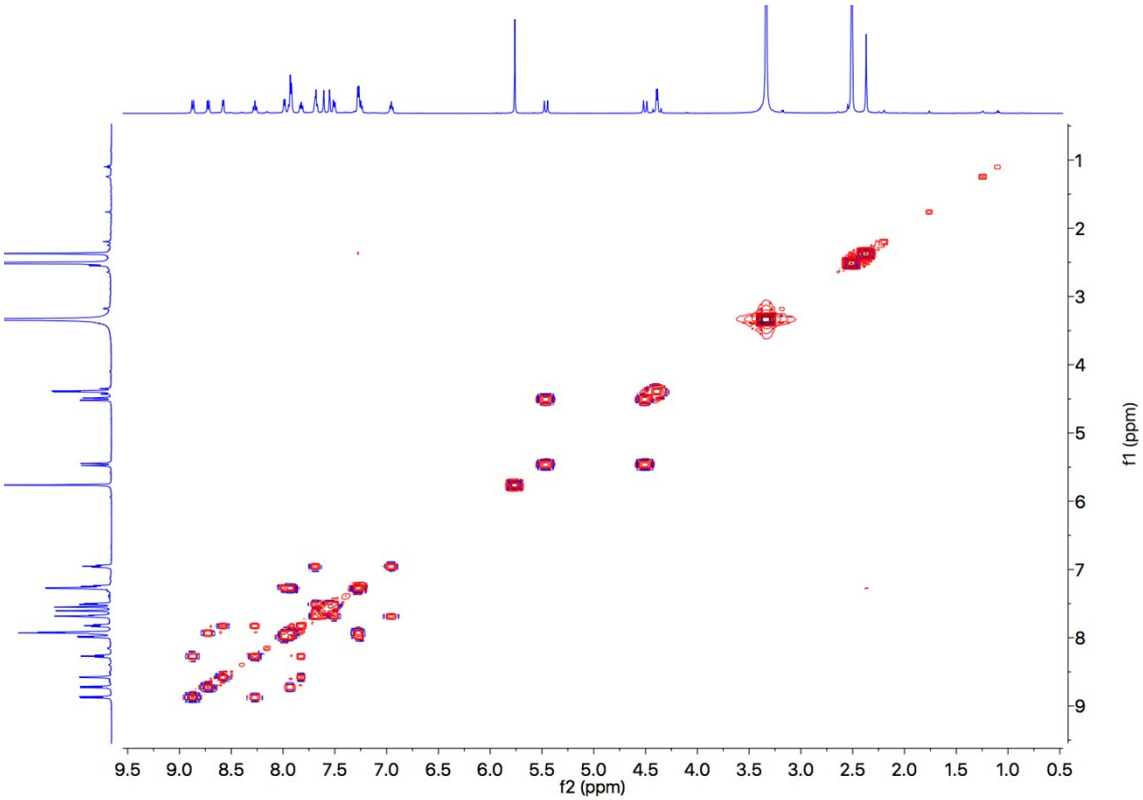

Figure S8. H-H COSY NMR spectrum of complex **2** in DMSO-d_6 at 298 K.

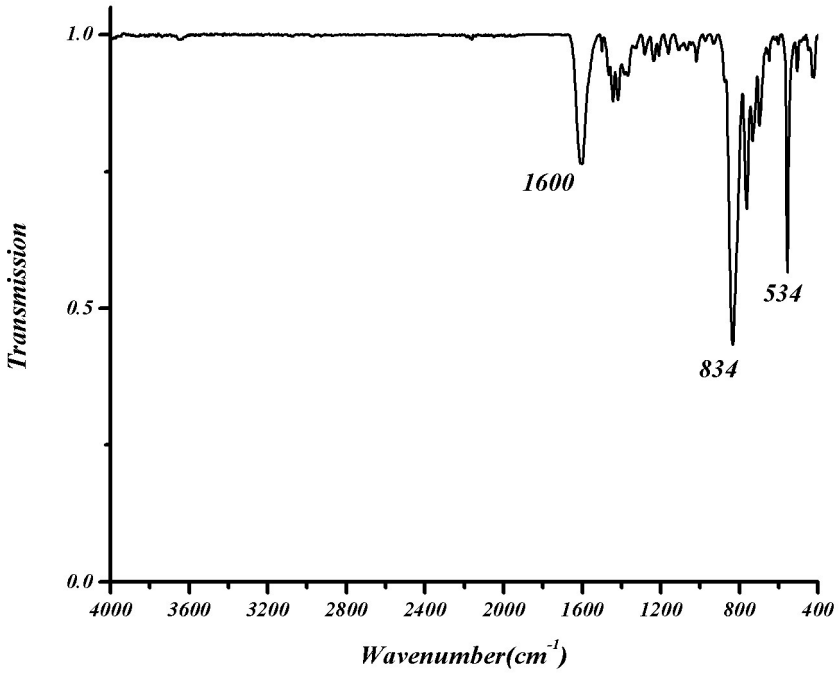

Figure S9. FT-IR of complex **2**.

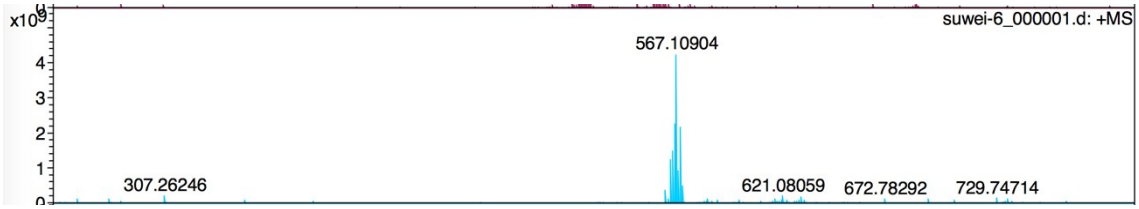

Figure S10. Mass spectrum of complex **2** in H_2O at positive mode.

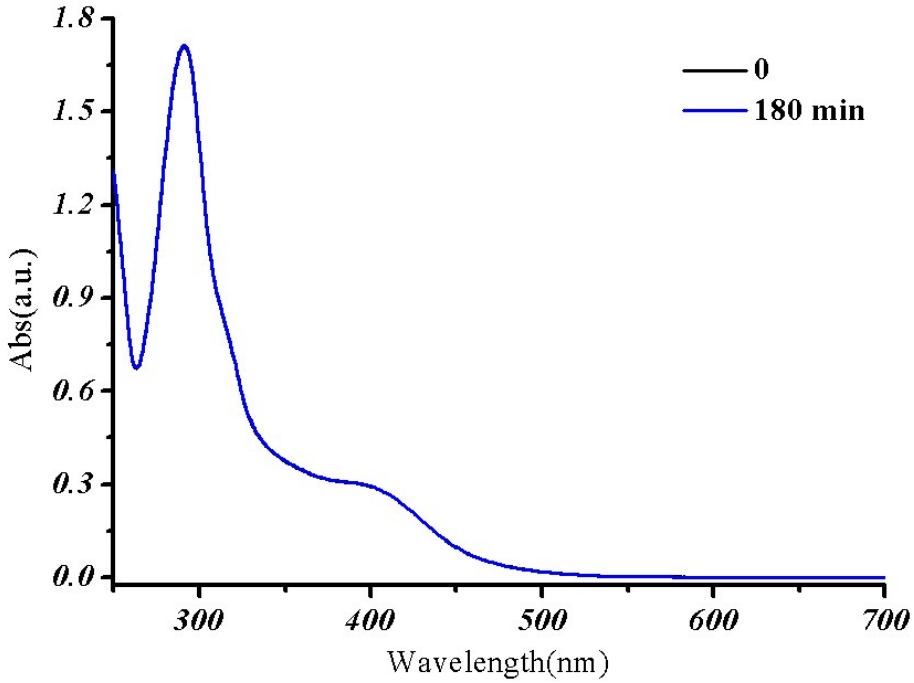

Figure S11. UV-Vis spectral changes of complex **1** in pH 1 aqueous solution (adjusted by CF_3SO_3H) over a period of 180 min.

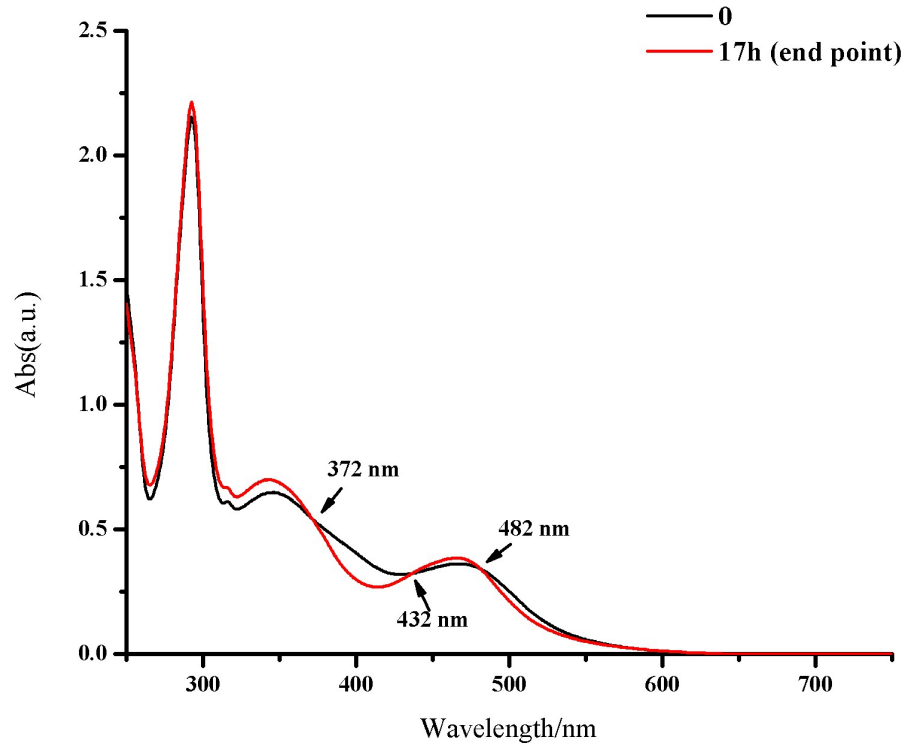

Figure S12. UV-Vis spectra of complex **2** and the species after complete transformation.

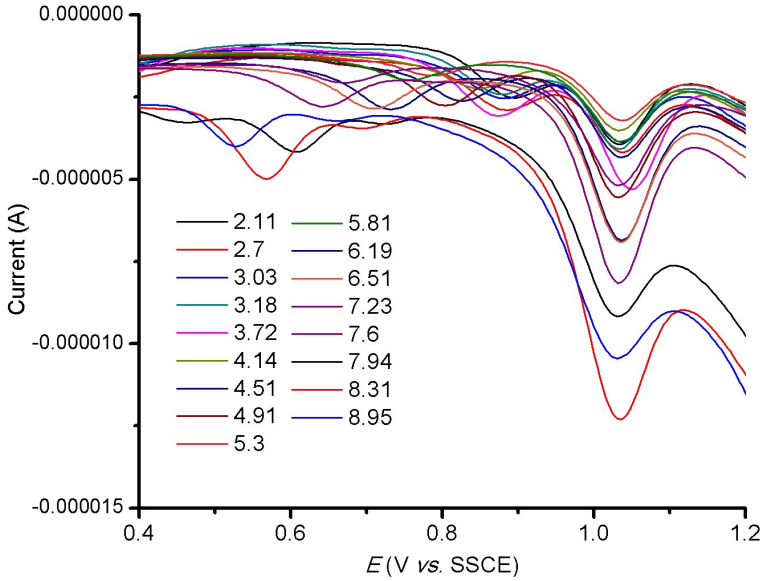

Figure S13. Differential pulse voltagrams for complex **1** at various of pH.

Table S1. Redox potentials of complex **1** and **2** in pH 1.0 CF_3SO_3H aqueous solution*.

Complex	$Ru^{III/II}$ (V)	$Ru^{IV/III}$ (V)	$Ru^{IV/II}$ (V)	$Ru^{V/IV}$ (V)
1	-	-	0.942	1.250
2	0.464	0.623	-	0.886

*Redox potentials were attained from differential pulse voltammetry.

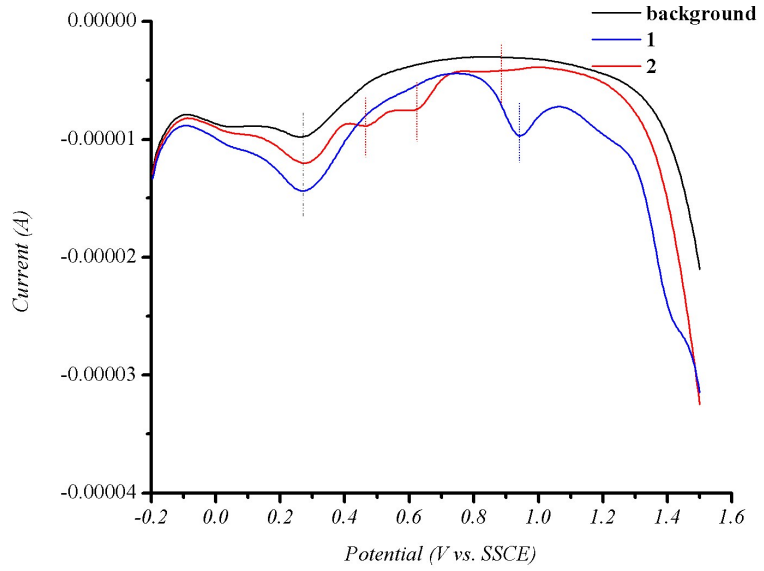

Figure S14. Differential pulse voltagrams for complex **1** and **2** in pH 1.0 CF_3SO_3H aqueous solution.

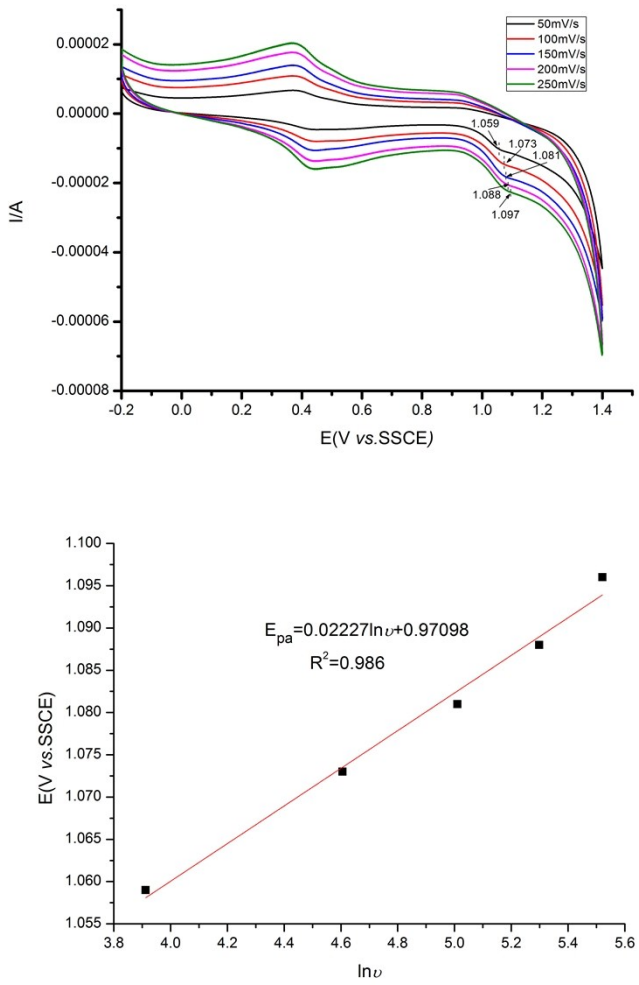

Figure S15. Top: cyclic voltammograms of complex **1** at different scan rates in pH 1.0 CF_3SO_3H aqueous solution. Bottom: linear fitting of E_{pa} *versus* lnυ.

Potential for redox couple at E_{pa} = 1.059 V (*vs*. SSCE, 50 mV/s) varied linearly with lnυ, according to the following equation[S1]:

$$E_{pa} = E^{\theta} + RT/(\alpha nF)\cdot\ln[RTk^{\theta}/(\alpha nF)] + [RT/(\alpha nF)]\cdot\ln\nu$$

α is transfer coefficient, k^{θ} is standard rate constant of the reaction, n is electron transfer number involved in the rate determining step, ν is the scan rate, and E^{θ} is formal potential, T = 298 K , R = 8.314 J·mol^{-1}·K^{-1}, and F = 96480 C·mol^{-1}. From the plot of E_{pa} versus lnν, a slope of 0.02227 was attained, which equals to RT/αnF. Thus, assuming that α is 0.5[S2], n = 2.28. This redox couple is a 2-electron redox process.

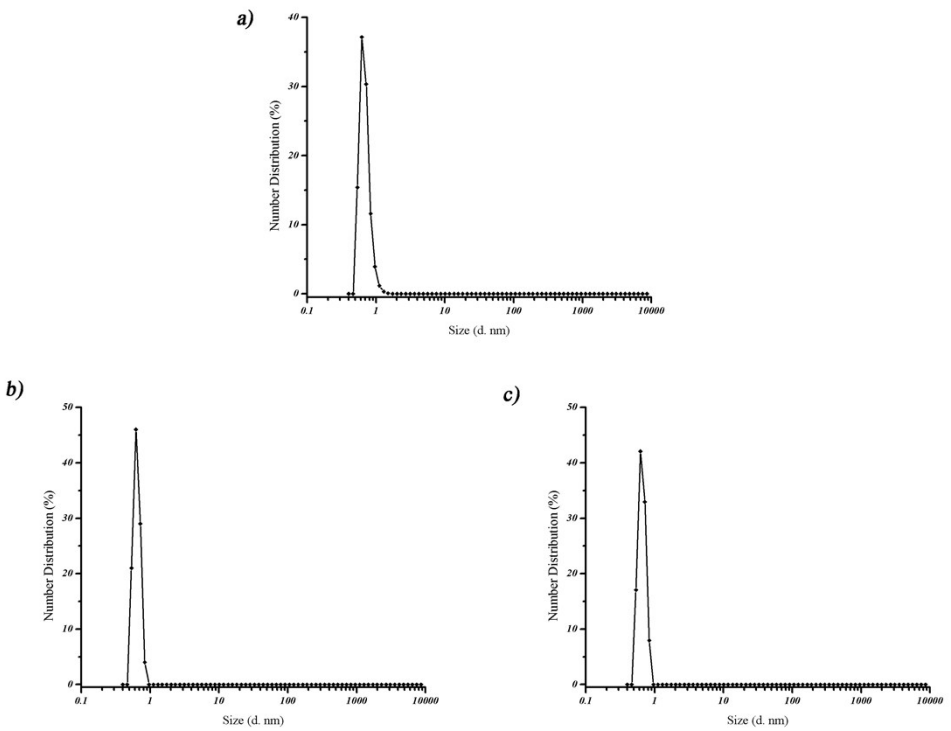

Figure S16. DLS measurements for (a) Ce^{IV} solution without catalysts and catalytic systems incorporating (b) complex **1** and (c) complex **2** after 3.5 h catalysis.

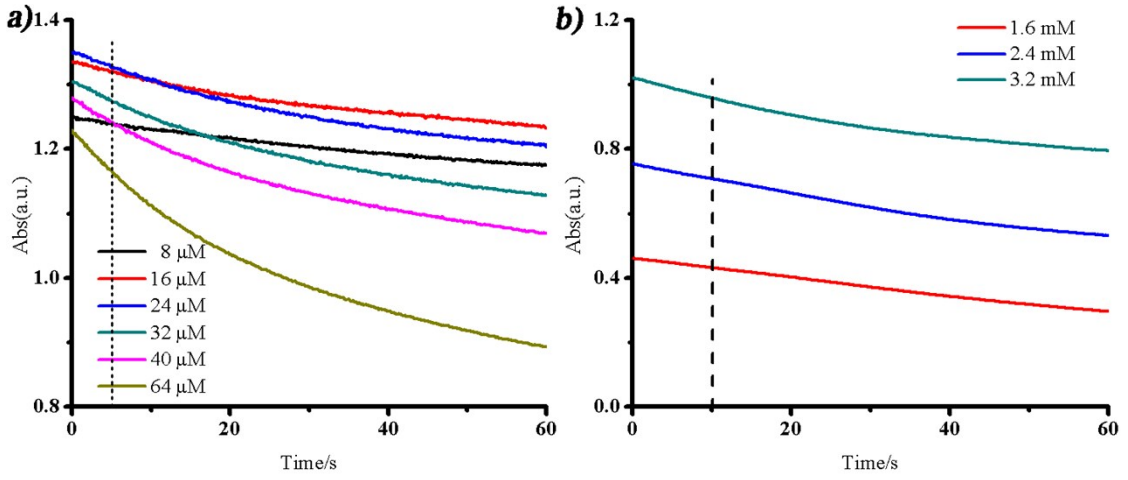

Figure S17. (a) Absorbance changes (360 nm) at various concentration of **1**. Conditions: initial [Ce^{IV}] = 3.2 mM, pH 1.05 CF_3SO_3H aqueous solution. (b) Absorbance changes (360 nm) at various concentration of [Ce^{IV}] in the presence of **1**. Conditions: initial [**1**] = 0.08 mM, pH 1.05 CF_3SO_3H aqueous solution.

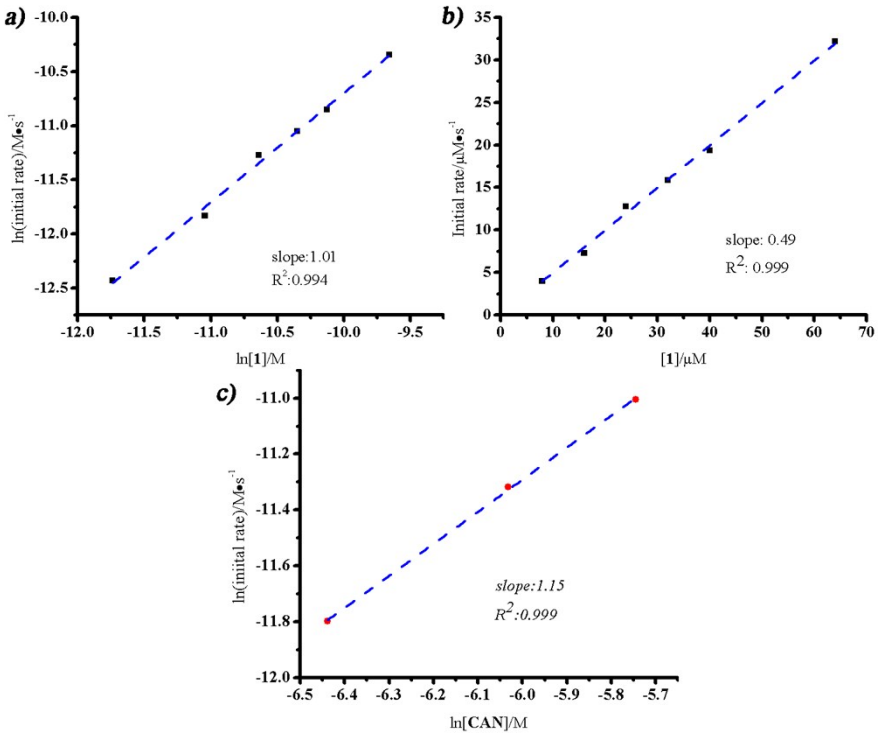

Figure S18. Kinetics data for [*Ce*^{IV}] catalysed by complex [**1**]PF_6 in pH 1.05 CF_3SO_3H aqueous solution. a) Natural logarithm of initial rate of [*Ce*^{IV}] consumption *versus* natural logarithm of concentration of [**1**]. b) Initial rate of [*Ce*^{IV}] consumption vs. concentration of [**1**]PF**6**. c) Natural logarithm of initial rate of [*Ce*^{IV}] consumption versus natural logarithm of concentration of [Ce^{IV}] in the presence of **1**.

It is known that concentrations of catalyst ([cat]) and oxidant ([Ce^{IV}]) play roles on the initial rate, thus the rate law of Ce^{IV} consumption could be expressed as :

$$\text{Initial rate} = k\cdot[\text{cat}]^m\cdot[\text{Ce}]^n,$$

$$\ln(\text{initial rate}) = \ln(K) + m\cdot\ln([\text{cat}]) + n\cdot\ln([\text{Ce}^{IV}])$$

herein, m and n are the orders of Ce^{IV} consumption (namely, water oxidation) depending on [cat] and [Ce^{IV}]. Therefore, from the plot of ln(initial rate) vs. ln([cat]) and ln(initial rate) vs. ln([Ce^{IV}]), we could know that the water oxidation at initial stage is of pseudo-first order on concentration of both complex **1** and Ce^{IV}.

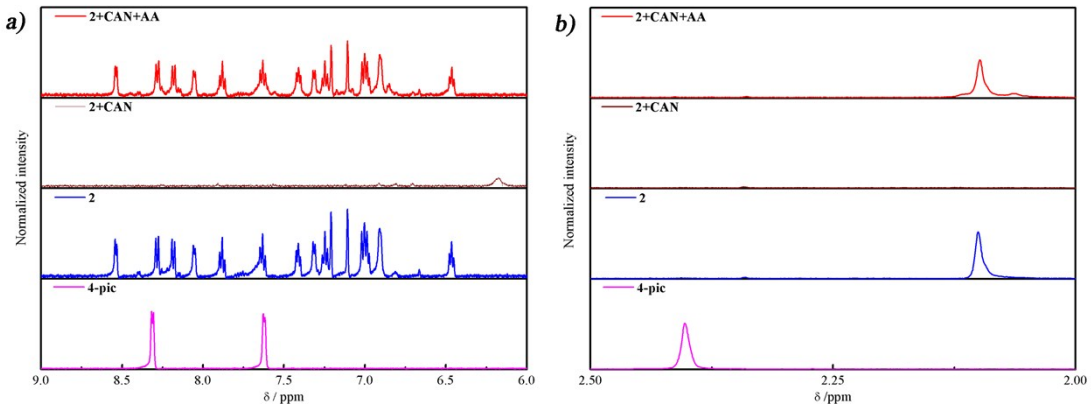

Figure S19. ^{1}H NMR spectral changes of complex **2** in (a) 6 – 10 ppm and (b) 2- 3 ppm titrated with *Ce*^{IV} and AA. Conditions: [**2**] = 10 mM, 70 equivalents of CF_3SO_3H, 0.5 mL D_2O.

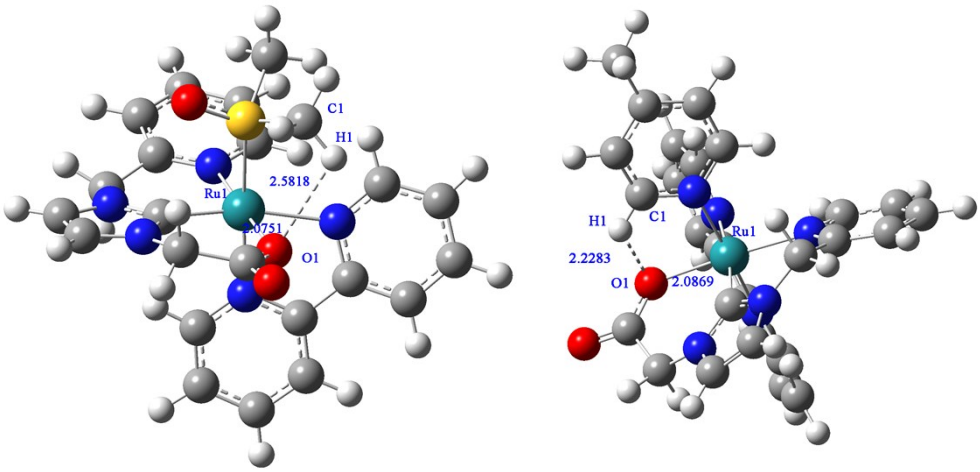

Figure S20. Calculated structures of complex $[\mathbf{1}]^+$ (left) and $[\mathbf{2}]^+$ (right).

Computational details. The geometry optimizations in the present study were performed using the Gaussian 09[S3] package and the B3LYP[S4] functional. 6-31G(d,p) basis set and 6-31G*(d,p) basis set were applied for the C,N, O, H, S elements for complex **2** and **1**, respectively. And the SDD[S5] pseudopotential was applied for Ru.

Table S2. Cartesian coordinates for $\mathbf{1}^+$.

Center Number	Atomic Number	Atomic Type	Coordinates(Angstroms)		
			X	Y	Z
1	6	0	-2.270193	-1.549502	1.373416
2	6	0	-3.001843	-2.692254	1.715608
3	6	0	-2.456861	-3.960032	1.535723
4	6	0	-1.164027	-4.049857	1.024186
5	6	0	-0.50876	-2.879483	0.665639
6	7	0	-1.043188	-1.640705	0.798683
7	1	0	-3.02225	-4.84825	1.799
8	1	0	-3.99455	-2.57835	2.138626
9	1	0	-0.669527	-5.006186	0.887901
10	1	0	0.487185	-2.906602	0.242942
11	6	0	-2.837122	-0.220488	1.842088
12	1	0	-3.913528	-0.341976	1.984502
13	1	0	-2.412877	-0.028865	2.839633
14	6	0	-3.483368	2.071622	1.061054

15	6	0	-1.543153	1.21446	0.252638
16	1	0	-4.40897	2.077475	1.615839
17	6	0	-2.890124	3.027663	0.308089
18	1	0	-3.209437	4.027816	0.058049
19	7	0	-2.642932	0.959984	1.014855
20	7	0	-1.699389	2.492257	-0.172299
21	6	0	-0.863511	3.203389	-1.150662
22	1	0	-0.776594	4.242107	-0.820266
23	1	0	-1.398456	3.206961	-2.108986
24	6	0	0.583874	2.7255	-1.443247
25	8	0	1.007056	1.556677	-1.060484
26	8	0	1.248959	3.514187	-2.099696
27	6	0	2.909187	-0.453557	0.38023
28	6	0	2.369798	-1.679638	-1.51151
29	6	0	4.274051	-0.640196	0.129287
30	6	0	3.706146	-1.915289	-1.816303
31	1	0	5.0187	-0.200695	0.781875
32	1	0	3.968138	-2.497815	-2.692897
33	6	0	2.410451	0.289586	1.556586
34	6	0	0.564907	1.186806	2.656382
35	6	0	3.246409	0.702621	2.601212
36	6	0	1.34074	1.622297	3.723584
37	1	0	-0.500299	1.378373	2.631372
38	1	0	4.308582	0.492319	2.567262
39	1	0	0.873231	2.144829	4.55166
40	7	0	1.960246	-0.960522	-0.451465
41	6	0	4.680246	-1.372444	-0.980776
42	1	0	5.735886	-1.513208	-1.188675
43	6	0	2.713139	1.376866	3.694121
44	1	0	3.356708	1.70175	4.505565
45	7	0	1.071928	0.53195	1.593339
46	44	0	-0.013389	0.001435	-0.141041

47	1	0	1.58788	-2.07844	-2.148183
48	8	0	-2.417922	0.270756	-2.394105
49	6	0	-0.003543	0.074274	-3.608974
50	1	0	-0.078994	-0.670917	-4.405652
51	1	0	-0.394775	1.03236	-3.959491
52	1	0	1.02151	0.206521	-3.261147
53	6	0	-1.366742	-2.156191	-2.620807
54	1	0	-0.42601	-2.708822	-2.677993
55	1	0	-2.013209	-2.585691	-1.852783
56	1	0	-1.882553	-2.166753	-3.583048
57	16	0	-1.084766	-0.400732	-2.192014

Table S3. Cartesian coordinates for **2**$^{+}$.

Center Number	Atomic Number	Atomic Type	Coordinates(Angstroms)		
			X	Y	Z
1	6	0	-0.616735	-2.351501	1.818391
2	6	0	-0.488975	-3.142584	2.961815
3	6	0	0.2489	-2.691998	4.053847
4	6	0	0.849545	-1.438573	3.963854
5	6	0	0.696256	-0.704276	2.795313
6	7	0	-0.017187	-1.13093	1.72371
7	1	0	0.349766	-3.302001	4.94535
8	1	0	-0.976183	-4.111693	2.991323
9	1	0	1.433061	-1.026989	4.780152
10	1	0	1.152579	0.271716	2.687664
11	6	0	-1.518846	-2.837219	0.697214
12	1	0	-1.794314	-3.875031	0.892217
13	1	0	-2.443892	-2.247385	0.702376
14	6	0	-1.063991	-3.717253	-1.650454
15	6	0	-0.316051	-1.645506	-1.091964
16	1	0	-1.538779	-4.673958	-1.499179

17	6	0	-0.507973	-3.165183	-2.758436
18	1	0	-0.391645	-3.557555	-3.756381
19	7	0	-0.929154	-2.772904	-0.634727
20	7	0	-0.054509	-1.897066	-2.401239
21	6	0	0.67965	-0.989736	-3.293708
22	1	0	0.366015	-1.196817	-4.316824
23	1	0	1.751332	-1.213227	-3.226538
24	6	0	0.50827	0.540747	-3.077999
25	8	0	0.234189	1.014538	-1.896885
26	8	0	0.694411	1.223757	-4.073869
27	6	0	2.864962	0.954564	0.130102
28	6	0	2.837293	-1.325976	-0.365425
29	6	0	4.263112	0.960598	0.062416
30	6	0	4.222561	-1.380313	-0.442126
31	1	0	2.231674	-2.209069	-0.528542
32	1	0	4.811432	1.87505	0.25118
33	1	0	4.71175	-2.322109	-0.66463
34	6	0	-0.025601	2.947395	1.103421
35	6	0	2.071574	2.145191	0.49745
36	6	0	0.45814	4.240788	1.268414
37	6	0	2.621364	3.424933	0.630769
38	1	0	-0.214527	5.035031	1.57237
39	1	0	3.668336	3.600168	0.416354
40	7	0	2.156846	-0.190705	-0.098318
41	7	0	0.750408	1.918001	0.724854
42	6	0	4.952123	-0.209695	-0.233164
43	1	0	6.035498	-0.209713	-0.289691
44	6	0	1.807717	4.484867	1.017677
45	1	0	2.220046	5.483669	1.1156
46	44	0	0.08427	0.004533	-0.076909
47	1	0	-1.072404	2.717351	1.265582
48	6	0	-2.739041	0.526834	1.108201

49	6	0	-2.612961	1.022546	-1.139851
50	6	0	-4.063326	0.939837	1.168373
51	1	0	-2.230774	0.166168	1.995507
52	6	0	-3.936043	1.448615	-1.152167
53	1	0	-1.989556	1.080428	-2.022543
54	1	0	-4.588279	0.895247	2.11782
55	1	0	-4.356672	1.818279	-2.082208
56	6	0	-4.706896	1.411536	0.015394
57	7	0	-2.004887	0.552737	-0.027563
58	6	0	-6.149849	1.838612	0.02995
59	1	0	-6.347202	2.603874	-0.725001
60	1	0	-6.802864	0.985353	-0.190535
61	1	0	-6.442765	2.229977	1.007739

Reference:

[S1] 1) H. S. Yin, Y. L .Zhou, S. Y. Ai, *J. Electroanal. Chem.*2009,**626**,80-88; 2) J. B. Raoof, A. Omrani, R. Ojani, F, Monfared, *J. Electroana. Chem*.2009,**633**,153-158; 3) E. Laviron, *J. Electroanal*. Chem. 1974,**52**,355–393.

[S2] A J. Bard, L R. Faulkner, Electrochemical Methods: Fundamentals and Applications, OXFORD UNIVERSITY PRESS, 1992.

[S3]. Gaussian 09, Revision D.01, M. J. Frisch, G. W. Trucks, H. B. Schlegel, G. E. Scuseria, M. A. Robb, J. R. Cheeseman, G. Scalmani, V. Barone, B. Mennucci, G. A. Petersson, H. Nakatsuji, M. Caricato, X. Li, H. P. Hratchian, A. F. Izmaylov, J. Bloino, G. Zheng, J. L. Sonnenberg, M. Hada, M. Ehara, K. Toyota, R. Fukuda, J. Hasegawa, M. Ishida, T. Nakajima, Y. Honda, O. Kitao, H. Nakai, T. Vreven, J. A. Montgomery, Jr., J. E. Peralta, F. Ogliaro, M. Bearpark, J. J. Heyd, E. Brothers, K. N. Kudin, V. N. Staroverov, T. Keith, R. Kobayashi, J. Normand, K. Raghavachari, A. Rendell, J. C. Burant, S. S. Iyengar, J. Tomasi, M. Cossi, N. Rega, J. M. Millam, M. Klene, J. E. Knox, J. B. Cross, V. Bakken, C. Adamo, J. Jaramillo, R. Gomperts, R. E. Stratmann, O. Yazyev, A. J. Austin, R. Cammi, C. Pomelli, J. W. Ochterski, R. L. Martin, K. Morokuma, V. G. Zakrzewski, G. A. Voth, P. Salvador, J. J. Dannenberg, S. Dapprich, A. D. Daniels, O. Farkas, J. B. Foresman, J. V. Ortiz, J. Cioslowski, and D. J. Fox, Gaussian, Inc., Wallingford CT, 2013.

[S4]. A. D. Becke, *J. Chem. Phys*. 1993, **98**, 5648-5652.

[S5]. D. Andrae, U. Häuβermann, M. Dolg, H. Stoll and H. Preuβ, *Theor. Chim. Acta*. 1990, **77**, 123-141.